MONITORING CELLULAR RESPONSE TO BIOMATERIALS

by

Ryan S. Czarny

A thesis submitted to the Faculty and Board of Trustees of the Colorado School of Mines in partial fulfillment of the requirements for the degree of Master of Science (Chemistry).

Golden, Colorado

Date: _____

Signed: _____
Ryan Czarny

Signed: _____
Dr. Melissa Krebs
Research Advisor

Signed: _____
Dr. Brian Trewyn
Masters Advisor

Golden, Colorado

Date: _____

Signed: _____
Dr. Bettina Voelker
Dean of Graduate Students
Department of Chemistry and Geochemistry

ABSTRACT

Cellular response, and monitoring that response, is a widely studied field and includes cellular interactions with inorganic, organic, and biological materials [1]. For the most part, cellular response studies examine the proliferation, differentiation, function, and migration of cells in various environments [2]. Viability and proliferation can indicate a stable cellular system, but that is not always the case. This study examines a new method that could be employed to measure the concentration of molecules present in a cellular environment that could influence their behavior.

The first part of this thesis examines the growth and differentiation of osteogenic cells on a bioglass product that was fabricated from recycled food waste products [3]. Multiple aspects of cellular response were monitored including their proliferation, viability, enzyme production, and mineral deposition while on the material and cultured under both standard and osteogenic conditions. Likely due to leaching of minerals from the bioglass product, the cellular differentiation response was difficult to interpret, and demonstrated that the microenvironments of the system needed to be taken into account. Thus, a new method for the detection of small molecules within a cell culture system was investigated to further study the cellular microenvironment, using pH-sensing nanofibers [5,6].

The second part of this thesis investigates the use of pH sensing nanofibers to observe the shift in pH of three dimensional hydrogel cell culture systems over time. *E. coli* was also introduced to the system to study how a simulated infection could cause a shift in pH and verify the response from the nanofibers. Throughout testing, the nanofibers performed as predicted, with an increase in fluorescence indicating a decrease in pH. This work sheds light on the

observation of cellular responses to their microenvironment and develops a new tool that could be used to monitor cell culture systems.

TABLE OF CONTENTS

LIST OF FIGURES

LIST OF TABLES

ACKNOEWLEDGEMENTS

I would like to thank Dr. Melissa Krebs, Dr. Renee Falconer, and Dr. Brian Trewyn in their support through these projects and developing a cohesive study. I would specifically like to thank Dr. Falconer for helping me throughout my Bachelors and transitioning me into my Masters work during my time at Mines. Additionally, I would like to thank Residence Life, specifically Elm Staff, for being my family and support through all of the ups and down of this research and work.

CHAPTER 1

INTRODUCTION

In medical history, there have been many advances that have improved the quality of life for the patients as well as improving the ability for medical practitioners to diagnose and treat disease. Since the 1980s, there have been improvements in invasive surgery, including the first fetal surgery performed in 1981 which allowed the medical practitioner to enter the uterus and remove a blockage in the fetus's bladder. Laparoscopic devices, developed in 1981, have improved minimally invasive surgery by allowing practitioners to place cameras on the end of the device to provide optic feedback to the surgeon. Improvements in transplant practices have also occurred, such as the first small bowel transplant in 1987 and the first face transplant in 2005, both of which took organs from donors and transitioned them to a new body [7]. All of these accomplishments pushed the medical field and medical technology forward, but almost all lacked a couple important aspects: acceptance to the body without any foreign body response and monitoring the system after it has been placed within the patient.

Since these early successes, new technologies have been developed to minimize foreign body response and allow continual monitoring within the system. The focus has moved away from taking existing materials from the host or a donor. Procedures have included autografts, allografts, and mechanical implants. Autografts take tissue from the host and extract it from one to site to place in another cause relief in one site and then morbidity in the other. Allografts are similar to autografts but the source of the tissue comes from another person and requires either a willing donor or post-mortem donor. Mechanical implants include those that are made from non-biological material that is simply placed in the body and is not integrated into the host's biology. Some recent advances implement stem cells taken directly from the donor, which can minimize,

if not eliminate, foreign body response [8]. Cells can be incorporated into a polymer scaffold, with or without bioactive factors, to create a three dimensional cell culture system [9]. After the system has been created, the material can be injected into the host or surgically placed within the host, depending on the procedure.

1.1 Bioglass

Glass has been used for many years in medical applications for prosthetics and other devices but it has typically come from standard glass that is made up largely from inorganic oxides, primarily silicon oxide. In past development, glasses were made from mineral extractions and recycled glass. This created a problem in that glass sources are not sustainable - only 10-20% of what is used to make new glass comes from recycled material, the rest comes directly from extracted mined materials [19]. In order to overcome this problem, a new source had to be explored, one that had a high concentration of inorganic oxides. Ivan Cornejo's lab started to look into the prospect of utilizing bio-waste for an oxide rich source [3]. There is an incredibly large amount of biological waste produced every year and, at this time, all of it is transported directly to landfills where it becomes the energy source of a widespread population of bacteria. As the bacteria are breaking down bio-waste, they produce carbon byproducts, mostly methane. Because landfills are not well contained, the methane often leaks and can easily contaminate the local environment. Incorporating this waste into glass not only adds to the total resource pool for glass production but also decreases the waste that would otherwise exist.

For the fabrication of glass from food waste, primarily the peels or shells of the food products are used (parts that are typically discarded that also have a high mineral content). The waste is collected and placed in a furnace between 400-1000 °C where it is turned into an ash

composite. At this point, different separation techniques can be implemented to extract the inorganic oxides out of the composite to be combined and solidified into the bioglass composite.

Figure 1.1 Diagram depicting the transition from raw food waste to the inorganic oxide powder and then on to the bioglass composite.

Bioglass is a specific type of glass composite composed of Na_2O, CaO, and SiO_2 that was originally investigated by Hench et al. [20]. One of the first creations of bioglass, in the 1970's, arose from the group's effort to build a new type of glass based on ceramic properties. Hench et al. was able to determine that different compositions of each chemical species (Na_2O, CaO, and SiO_2) produced different cellular responses to the bioglass. The composition could be tuned to be a better site for bone bonding, non-bone bonding, soft tissue bonding, and multiple other options. Cornejo pursued a composition that would stimulate bone binding with the hope of prosthetics implementation. Taking different components from the different food waste products, including peanut shells, egg shells, banana peels, and other sources, the Cornejo lab created a crystalline composite that fell within the range set forth by Hench's research. The average % range of each of the inorganic oxides are (percent by mass): SiO_2- 0-55%, CaO- 22-27%, K_2O- 0-9%, Na_2O- 6-

24%, MgO- 0-8%, P_2O_5- 1-3%, and B_2O_3- 0-51%. Based on previous research, Cornejo's groups aimed to create bioglass that contain about 45% SiO_2 and roughly equal parts of CaO and Na_2O.

1.2 Alginate

To compensate for foreign body response that occurs frequently in the medical field, bio-polymers and other bio-materials have been tested and utilized, most commonly alginate [10]. Alginate is a biopolymer that is extracted from seaweed and is composed of ether linked chains that contain carboxylic acids and alcohol groups (Figure 2)[11]. In solution, alginate can be combined with $CaCl_2$, $CaSO_4$, or other activators to initiate the crosslinking of polymer chains, with the calcium chloride producing immediate polymerization because of its high solubility and calcium sulfate being a slower polymerization because of its low solubility [12]. The crosslinking occurs due to the divalent calcium atoms in solution. The calcium is attracted by carboxylic acid groups from different alginate polymers and forms a ladder-style structure as the pattern repeats to the end of the chains [13]. There is no covalent bonding that occurs between the polymers, but rather strong charge interactions. Once the crosslinking has occurred, a hydrogel is formed encapsulating a large volume of water within the network.

The mechanical strength of the polymer and the pore size can be tuned in order to provide different properties based on the methods and conditions in which the hydrogel is created [14]. For example, pore size for these gels can be adjusted based on ionic character of the cross-linking cation along with other chemicals that are in solution with both the alginate and the cations [15]. Pore size can also be adjusted through freeze-thaw techniques and lyophilization processes. Changes in features such as pore size can cause differences in durability as well as the release profile that the gel has in drug delivery. Because of its charge interaction cross-linking, the hydrogel will naturally degrade over time simply by being in a biological system. The body

has a relatively low level of calcium (2.5 mmol/L) in comparison to the hypertonic hydrogel and will promote the diffusion of calcium into the system, thereby degrading the hydrogel network in the same process [16].

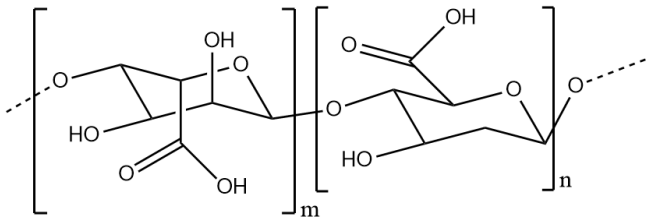

Figure 1.2 Chemical Composition of Alginate polymer

To be able to use alginate with anchorage dependent cells embedded within the polymer network, the alginate has to be modified with a cell-adhesive peptide containing arginine-glycine-aspartic acid (RGD) [17]. A depiction of the modified polymer can be seen below in Figure 3. In order for this reaction to occur, first, 1-Ethyl-3-(3-dimethylaminopropyl) carbodiimide (EDC) goes through a substitution reaction with the hydrogen on the alcohol group from the carboxylic acid group on the n group of the alginate chain. After that, the RGD peptide preforms an electrophilic attack on the carbonyl carbon to form an amine bond. The addition of RGD to alginate for biological interactions is widely used throughout the bioscience community and has been used in multiple tests of hydrogel as a cellular holder and scaffold. Because the scaffold promotes the adhesion of the cells to the matrix, the cells are able to adhere and proliferate into the system [18]. As the hydrogels degrade over time, the cells will secrete extracellular matrix (ECM) molecules and replace the degrading material.

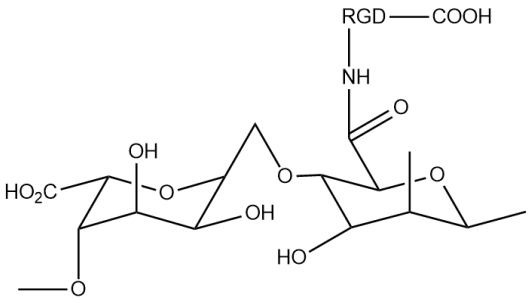

Figure 1.3 RGD-modified alginate.

1.3 Nanosensors

The use of nanosensors has been extensively studied within the field of biochemistry and has the potential to reshape how biological systems are observed and analyzed. Clark's lab at Northeastern University first looked into pH sensitive chromoionophores [21,22]. Early tests identified ionophores that would respond to specific pH values. In order to contain the species, the ionophore was placed within a matrix containing a multitude of materials to capture it within its environment. They calculated the intensity of the chromoionophore emission as a response of pH which opened up new areas of pH identification beyond the standard lab bench probe. Further work with these chromoionophores led to their use as sensors throughout a biological system, providing the ability for researchers to inject these chemical species alongside their intended drug and track the movement of the fluid and molecules as they penetrated the system *in vivo* [23]. One such study focused in on histamine after it was injected into a rat. Histamine and a tag enzyme were mixed together and placed in different locations along the spine of the rats. Images were taken at multiple time points to determine the fluorescence. New insight was gained as to how the body mobilizes drugs and how the drugs naturally perpetuate throughout the system. Since its first implementation, this method of following chemical species through the use of chromoionophores has been used in a wide array of applications ranging from ion

transport across membranes, amino acid binding tracks, and with other biomolecules including glucose in a system [24,22].

The use of nano-optodes, or nanomaterial optical devices, is ideal for biological systems because the specific chromoionophore can be chosen so that it will provide an explicit excitation and emission spectra that can be used in identification. This not only allows for little to no interference from the biological system at the given wavelengths but also permits multiple chromoionophores to be used within one system to monitor and detect multiple variables at one time. The different wavelengths can also be used as cross-references to one another based on their intensity to create a normalized quantity.

Since the initial development of optodes as a method of detection, the chromoionophores have also been incorporated into a nanofibrous matrix in order to retain their durability and increase their effective life-time [25]. Some work in this area included detecting calcium concentrations within a biological system [6]. The fibers proved to be biocompatible and provided the desired fluorescence response needed to prove the movement of the hydrogen ions for sensing.

CHAPTER 2

BIOGLASS

Bioglass is a unique material that has very specific compositional requirements. The name bioglass does not denote that the glass is made from biological materials but rather that the material is suitable for life to reside. This project looked into how life interacts with the bioglass.

2.1 Bioglass Materials and Methods

Bioglass samples were collected from Dr. Ivan Cornejo's lab in the Metallurgical and Materials Engineering Department at the Colorado School of Mines. Each of the bioglass samples were 25.4 mm in diameter, 0.1 mm thick, and were polished with 1200 grit SiC paper to reduce roughness to below 10 µm. The bioglass was placed in empty micropipette containers and sterilized by autoclaving. Coverslips that were 10 mm in diameter made from manufactured glass were sterilized in the same fashion.

MC3T3s, an osteoblast precursor cell line, were cultured on Tissue Culture (TC) plates in densities of about 1-2 million cells per plate. The cells were supplemented with α-Minimal Essential Media (α-MEM) with 10% fetal bovine serum (FBS) and were allowed to proliferate for 1 week, or until confluent, before passaging the cells. α-MEM+ was made with supplemental osteogenic factors including 1% v/v 10^{-5} M dexamethasone, 1% v/v 200 mM β-Glycerophosphate (BGP), and 1% v/v ascorbic acid-2 phosphate added to α-MEM. This osteogenic media was used to promote the differentiation of MC3T3s down the osteogenic lineage [26].

Before the introduction of bioglass to the system, a test was run to determine the differing effects of α-MEM in comparison to α-MEM+ as well as to determine how the introduction of

glass to the system would change cellular behavior. A 6 well plate was set up with α-MEM+ and α-MEM with cover glass without cells in the first row, α-MEM+ with and without coverslips and with cells in the second row, and α-MEM with and without coverslips and with cells in the third row. A representation of the plate can be seen in Figure 4. This setup was designed as a set of 4 to accommodate the short and long term assay, alkaline phosphatase assay, DNA assay, and calcium deposition assay. Data was collected for each of the tests and analyzed.

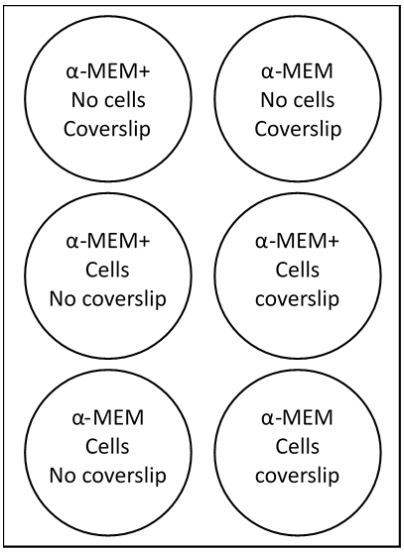

Figure 2.1 Setup for comparison test to determine effects of media and glass of cell growth.

In sterile conditions, bioglass samples were placed in non-TC 6-well plates for one column of the plate, or a total of three bioglass samples in a 6-well plate. Cover slips were placed in the remaining three wells within the well plate as can be seen in Figure 5.

After the different types of glasses were placed in the wells, MC3T3s were placed on top of each of the glass pieces at a concentration of 40,000 cells per glass slide. Once the cells had been deposited on top of the glass, they were allowed to sit for 20 minutes in order to obtain early stages of attachment to the glass surface.

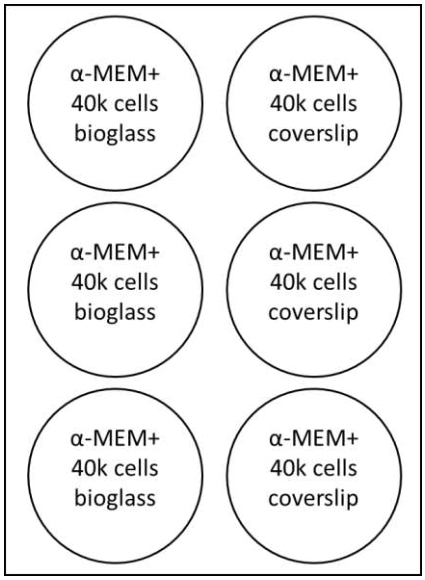

Figure 2.2 Diagram for the setup of the comparison between bioglass and manufactured glass.

After 20 minutes, 2-3 mL of α-MEM+ was added to each well until the media covered the slides and allowed them to be completely submerged. The plates were then placed in an incubator at 37° C and 5% CO_2 concentration. This setup was again done in sets of four to account for the different assays on the glasses including, short and long term viability, alkaline phosphatase production, calcium deposition, and DNA concentration. Media was changed every 2-3 days as is consistent with MC3T3 cell culturing.

The short term viability assay was taken at the one-week mark using a live/dead staining. Residual media was syphoned out of the wells and 1 mL of new α-MEM+ was added back into the well. The viability assay included the following: 200 µL of dimethyl sulfoxide (DMSO), 100 µL of ethidium bromide, and 60 µL of phosphate buffered saline (PBS) solution [27]. This solution was added at 50 µL of assay dye solution per 1 mL of α-MEM+ solution into the well. The resulting solution was allowed to sit for 5 minutes to permit the staining solution to permeate and dye the cells present. After the sit time had elapsed, 300 µL of the solution was taken from each of the wells and placed in 96 well plates in duplicates.

Another viability assay used included the 3-(4,5-dimethylthiazol-2-yl)-5-(3-carboxymethoxyphenyl)-2-(4-sulfophenyl)-2H-tetrazolium (MTS) assay and protocol. The MTS assay is composed of 20 % CellTiller, 1% Penicillin, and 79% α-MEM+ solution [28]. The wells were washed 3 times with PBS solution and 500 µL of the MTS solution was added to each of the wells. The plate was placed in the dark on a rotating plate for 90 minutes to allow for the mitochondrial protein to be stained. Two sets of 100 µL of the resulting solution was extracted and placed in a 96 well plate for analysis at an absorbance of 490 nm. MTS assays have some quantitative analysis associated with them; however, the assay is typically used as a comparison between different samples, as it was for this test.

The alkaline phosphatase assay took place at the two week mark when the enzyme should be at its highest level in production [29]. Alkaline phosphatase is an enzyme that gives insight into the osteogenic nature of the cells and how well they are proliferating on that lineage. In order to make sure that the enzyme went into solution, 300 µL of Celytic M was added to each of the wells and a cell scraper was used on all of the glass pieces. 100 µL of the above solution was taken and placed in a 96 well plate along with 100 µL of the dye. This solution was placed in an incubator for 30 minutes at 37° C, before 50 µL of 0.1 M NaOH was added to each of the wells to stop the reaction. A standard curve was created using p-nitrophenol at 0, 25, 50, 100, and 200 µM and the solutions treated the same as above. The absorbance was read at 410 nm.

For the calcium deposition assay that occurred three weeks into the experiment, 1 M acetic acid was added to the wells at equal parts to the water suspension already in the wells [30]. A sample of 50 µL of solution was extracted from each of the wells and placed into a 96 well plate. A solution of equal parts buffer, PBS, and binding reagent, from the BioVision Calcium Colorimetric Assay Kit, was mixed and 200 µL of the resulting solution was added to a 96 well

plate [31]. This combined solution was allowed to sit for 30 minutes for the reaction to fully occur. Standard solutions were made at 0, 25, 50, 100, and 200 µg/mL of calcium chloride in distilled water, and were placed in the 96 well plate. The plate was run at an absorbance of 560 nm.

The DNA concentration assay was done in conjunction with the calcium concentration, at week three, using the PicoGreen dsDNA Assay Kit from Life Technologies [32]. For this assay, a standard buffer from the kit was used with the total needed solution split in half into two different falcon tubes, one for the samples and one for the dye. For the solution for the dye, a 1:200 dilution of the dye was made and the tube was placed in a dark location. A standard solution of DNA was pre-prepared with concentrations at 0, 0.1, 0.3, 1, and 3 µg/ mL. 107 µL of the solution for the buffer was placed in each sample well within the 96 well plate. 43 µL of the sample (the same solution that was cell scraped in the above assay) was added to the well, as well as 150 µL of the dye-buffer solution. The solution was allowed to sit for 5 minutes with the absorbance taken at 460 nm.

2.2 Bioglass Results and Discussion

The comparison of MC3T3s grown in a well plate versus those that were cultured on top of coverslip glass was first analyzed. Images were taken at 40x magnification in white light for the two different conditions (with and without the coverslip) after 1 week of culturing. Images of this test can be seen in Figure 6. The pictures show the cells are proliferating at a much higher rate on the glass than on the non-TC well.

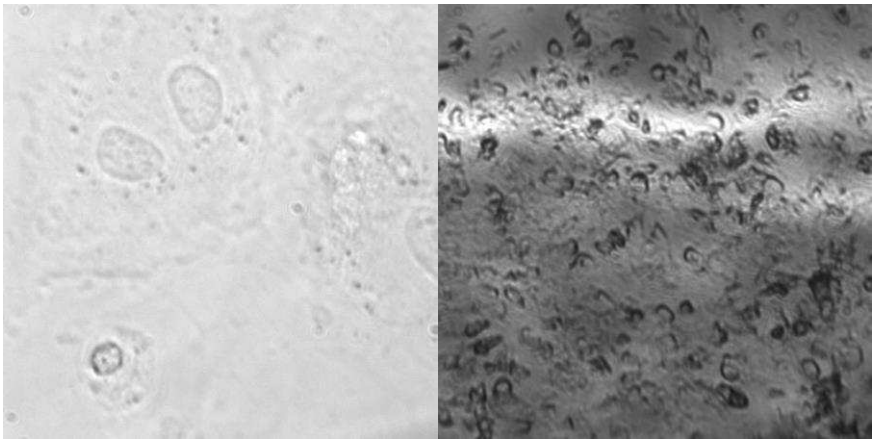

Figure 2.3 Comparison of MC3T3s in a non-TC well plate (to the left) and those cultured on a cover slip (to the right).

Along with qualitative pictures, a MTS assay, which measures mitochondrial activity of cells and can be correlated to cell numbers and viability, was conducted to determine the presence of the cells after 4 weeks from the initial seeding. Both of the media samples were used as a blank and adjusted to a zero value and the difference taken out of the value for each of the other samples. The data showed the cells cultured in osteogenic media (α-MEM+) had greater metabolic activity in comparison to the cells with the baseline media (α-MEM). In addition, the MC3T3 cells had greater metabolic activity when they were seeded on coverslips that allowed them to adhere to the surface, as opposed to the well plate (Table 1).

Table 2.1 Proliferation data for comparison of osteogenic and non-osteogenic media as well as between regular well plates and those with coverslips added.

Sample	Corrected Abs.
MEM+	0.000
MEM+ Cells	0.070
MEM+ Cell Glass	0.095

MEM	0.000
MEM Cells	0.013
MEM Cells Glass	0.003

After determining there was value in using coverslips, and therefore glass, the focus of the experiment shifted to looking at the difference between coverslips and bioglass in terms of the proliferation and differentiation response of the cells. At the 1-week point, a MTS viability assay was conducted; however, the data file containing all of the information became corrupt and therefore the tests results were lost and produced no usable data. Instead, visual inspection determined that the bioglass had a noticeably higher concentration of cells when compared to the coverslips.

The extent of osteogenic differentiation of the MC3T3s was measured. After two weeks of culture, the alkaline phosphatase concentration was determined for the cells cultured on bioglass and coverslips. The data is shown in Figure 7. The bioglass samples had, on average, lower production of alkaline phosphatase enzyme compared to the coverslips. According to the assay data, the bioglass system had less alkaline phosphatase activity indicating and lower osteogenic activity compared to the regular glass when normalized to the DNA taken at week 2. The average value of enzyme concentration for the bioglass was 13.675 µg/mL of alkaline phosphatase per µg/mL of DNA and for the coverslips 0.266 µg/mL. This assay is not an indication of how many cells were present on each of the glass types but rather serves to show how well the MC3T3s were functioning as osteoblasts. Statistical analysis, using an Unpaired t-test, showed a P-value of $P = 0.0009$ indicating the two sets of data are significantly different from one another. The supporting data for this can be seen below in Table 2.

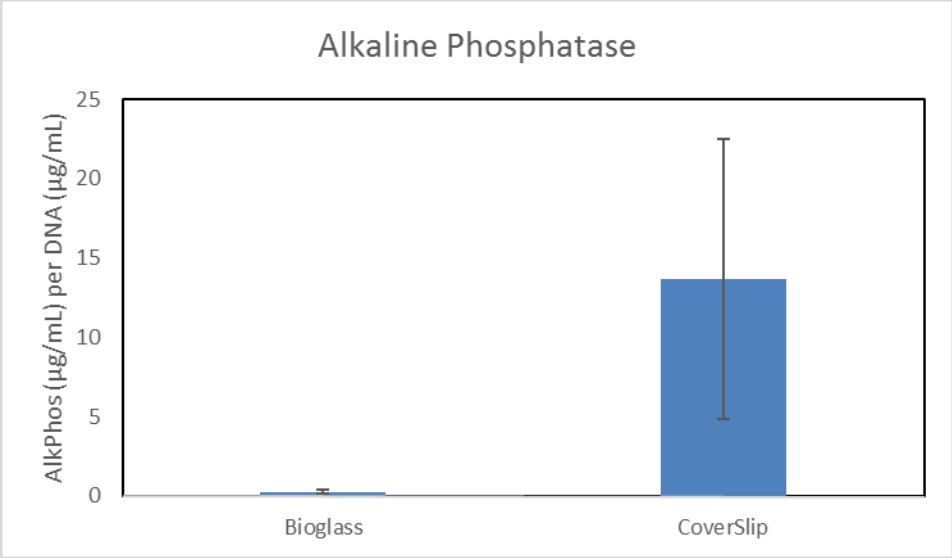

Figure 2.4 Data analysis of the concentration (µg/mL) of alkaline phosphatase normalized to DNA concentration (µg/mL, data taken at week 2) present between bioglass and coverslips.

Table 2.2 Statistical analysis of the alkaline phosphatase production of the bioglass and coverslip.

Parameter:	Bioglass	Coverslip
Mean:	0.2666	13.675
# of points	3	3
Std deviation:	0.1242	5.77
Std error:	0.07168	3.331
Minimum:	0.1397	7.497
Maximum:	0.3878	18.925
Median:	0.2723	14.601
Lower 95% CI:	-0.04185	-0.6605
Upper 95% CI:	0.575	28.009

Next, the calcium deposition and the DNA concentration were observed at the 3-week point. The calcium deposition, when taken by itself, showed cells on the bioglass had a much higher concentration at 165.67 µg/mL calcium in comparison to 74.70 µg/mL of calcium deposited by the cells on the coverslips. At first, this data appeared contradictory to the alkaline phosphatase activity seen at 2 weeks. Previous research suggests alkaline phosphatase should directly correlate to the concentration of calcium deposited by the cells [33]. One explanation,

however, was to consider the DNA concentration of the samples, with the bioglass samples measuring 17.50 µg/mL of DNA while the coverslip samples measured 2.17 µg/mL of DNA. The calcium data, when normalized to the DNA, resulted in a value of 14.096 µg Ca/µg DNA for the bioglass and 1.544 µg Ca/µg DNA for the coverslips, which still contradicted what would be expected. The normalized values for the calcium deposition can be seen in Figure 8. Statistical analysis was run on the two sets of data and the P-value again came out to be 0.0009 which indicated that the two sets of data are significantly different from one another. The analytics values are shown in Table 3.

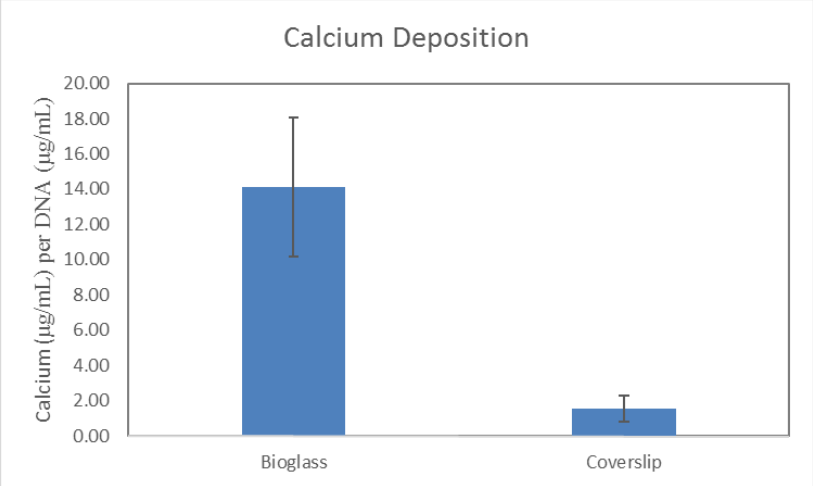

Figure 2.5 Data analysis of the concentration of calcium (week 3) normalized to DNA (µg Ca/µg DNA) present between bioglass and coverslips.

Table 2.3 Statistical analysis of the calcium deposition of the bioglass and coverslip.

Parameter:	Bioglass	Coverslip
Mean:	14.096	1.544
# of points:	3	3
Std deviation:	2.436	0.3083
Std error:	1.407	0.178
Minimum:	12.251	1.327
Maximum:	16.857	1.897
Median:	13.179	1.408
Lower 95% CI:	8.043	0.7784
Upper 95% CI:	20.148	2.31

At the 4-week point, the long term viability of the samples was measured using the MTS assay. All of the values were normalized to the lowest value, which in this case is the cell count from a coverslip well. The bioglass cells had a viability of 114.03% in comparison to the coverslips which had a relative viability of 104.35%. Overall, this suggests that the MC3T3s prefer the bioglass to the coverslip in terms of proliferation (Figure 9).

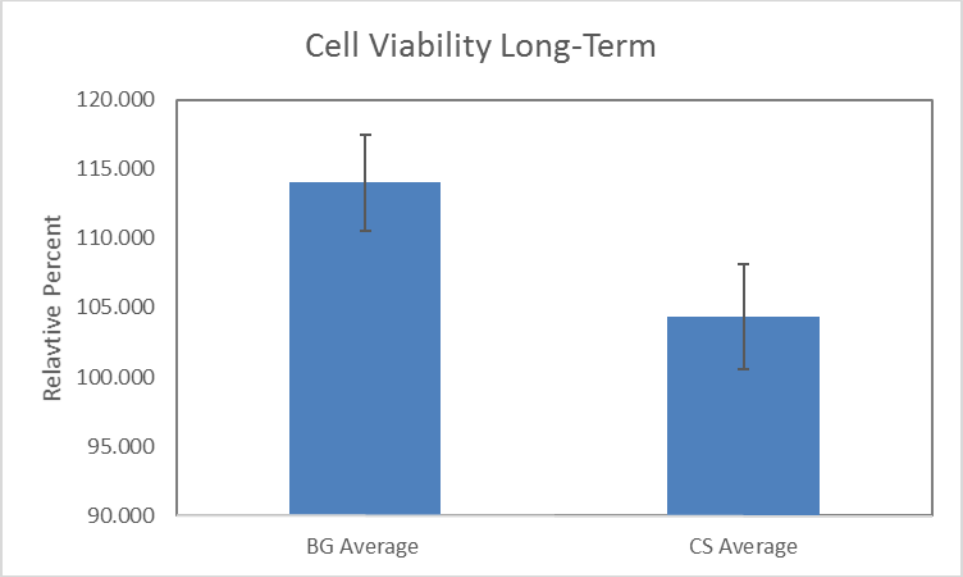

Figure 2.6 Viability comparison between the bioglass and coverslips using a baseline of a coverslip value to determine the relative viability.

An Unpaired t-test was run on the data which showed no statistical difference between the two with a P-value of 0.2574. This value does not allow for the null hypothesis of the two sets of data being the same to be rejected. The data for the statistical analysis can be seen in Table 4. Though they are not statistically different, the data does show a general trend to more cells present on the bioglass than on the coverslip, which coincides with the DNA data collected at the 3-week time point.

Table 2.4 Statistical data for the viability assay (MTS) for bioglass in comparison to coverslips.

Parameter:	Bioglass	Coverslip
Mean:	114.03	106.19
# of points:	6	6
Std deviation:	9.306	5.4
Std error:	3.799	2.204
Minimum:	105.15	100
Maximum:	131.76	112.56
Median:	111.19	106.52
Lower 95% CI:	104.26	100.52
Upper 95% CI:	123.79	111.85

By compiling the data from the four tests, a larger-scale view of what was occurring with the cells on both the bioglass and the coverslip can be considered. The data for the alkaline phosphatase enzyme and calcium deposition (when normalized to the DNA concentration) do not correlate to one another showing there were other factors at work. Both the DNA concentration assay as well as the long term viability assay indicate there were more cells present on the bioglass even though they were not behaving osteopathically. As the cells have to choose which path to take, differentiation or proliferation, the MC3T3s that were on the bioglass appeared to continue on the proliferation pathway while those on the coverslip appeared to move down the differentiation pathway. MC3T3s will either choose to continue to divide and proliferate within a system, as was seen on the bioglass, or they will halt their division pathway and focus on the maturation of their extracellular matrix, as was seen on the coverslip. Based on literature on this topic, the two different pathways that the cells took, proliferation and differentiation, match what is expected as far as gene expression with the alkaline phosphatase but contradicted what was expected for the calcium deposition [34]. One possible contribution to the high calcium levels measured in the bioglass samples could be leaching of calcium ions from the bioglass, contributing to these higher measurements. Not only could the calcium directly contribute to the calcium measurements, but it could be affecting how the osteogenic cells are responding in terms

of their alkaline phosphatase expression and proliferation. More research is needed to determine the extent of calcium leaching from the bioglass over time.

This disconnect between the expectation of low calcium deposition on bioglass due to the fact that they appeared to be undifferentiated cells sparked an interest in what was occurring with the cells on a micro-environmental level. Knowing what happens on the cellular level would help determine what pathways where occurring or if some other factor was at work. For example, bioglass may have been the cause of calcium leaching into the system, thereby skewing the results that were collected.

Initially, a set of experiments was created to determine the influence of calcium on the MC3T3s to see if their ambient environment determined whether or not they chose proliferation or differentiation. Unfortunately, the source of bioglass was discontinued so no further work with that specific material could be undertaken.

To continue learning more about the system, a collaboration was started with Dr. Heather Clark at Northeastern University. This new project used pH sensing nanofibers to observe and analyze the microenvironments in a biological system.

CHAPTER 3

PH-SENSING NANOFIBERS

In order to examine the microenvironment of cultured cells, poly-(ε-caprolactone) (PCL) pH-detecting nanofibers were fabricated by collaborators at Northeastern University. Previous results on the bioglass suggest what is happening on the large-scale level can differ from what is happing on the cellular level and therefore lead to very different results.

Previous research has looked into the microenvironments of cellular systems through the use of sensor nanoparticles. Typically injected with drugs, the nanoparticles fluoresce throughout the biological system allowing the drugs to be tracked and the pathway by which the drug travels throughout the body can be determined [23]. Much work has already been done in this area, specifically within rats, to follow the movement of drugs through the living system and observe how injections diffuse in the rat tissue.

The benefit to using nanofibers is they allow the study of a specific location so one can monitor the microenvironment of that biological system. In order to provide the needed information, two dyes are placed within the nanofibers, with one dye serving as a reference and the other as an indicator of the pH. Each of the dyes has different excitation and emissions and therefore can be imaged distinctly within the sample. The normalized quotient of the two emissions can be used to give information on the pH of the microenvironment of the biological system.

The working hypothesis for this project was the nanofibers would fluoresce with a greater intensity in acidic environments, and thus provide data about the relative pH of cellular systems.

3.1 pH nanofibers Methods and Materials

Preliminary tests were done to the anticipated system to make sure little or no effect from the setup incorporating the pH nanofibers would occur. In preparation for the testing, sterile alginate and calcium sulfate were created through the following methods. 9.758 g of 2-(N-morpholino) ethanesulfonic acid (MES) and 8.771 g of sodium chloride were added to 470 mL of nano-pure water in a 1-liter sterile beaker. The pH of the solution was adjusted to 6.5 with 1 M NaOH and 4 M NaOH, 2 mL of the solution were put aside and the remaining solution filtered with a 0.22 µm vacuum bottom-top filter. At this point, 4.995 g of alginate was added to the solution to make it 1% weight per volume. The solution was allowed to sit overnight. A mass of 136.6 mg of N-hydroxysulfosuccinimide (sulfo-NHS) was added to the total solution along with 242.8 mg of 1-ethyl-3-(3-dimethylaminopropyl) carbodiimide (EDC) and allowed to sit at room temperature for 30 minutes. 63.3 mg of RGD peptide was dissolved in the saved 2 mL of solution set aside and added to the full solution which was allowed to sit for 20 hours [35]. A mass of 89.5 mg of hydroxylamine was added to the solution to quench the reaction and the final solution was placed in dialysis tubing in nano-pure water in a plastic tub. The nano-pure water was changed twice a day for 4 days. The solution was transferred from the dialysis tubing into a beaker and filtered through a 0.22 µm filter.

Aliquots of approximately 150 mL were removed and frozen overnight. The frozen solutions were placed on the lyophilizer and allowed to sit for 2 weeks to completely dehydrate. The dehydrated solutions were placed in the freezer to await hydration for use. The purified and sterile alginate was then added to α-MEM at a volume to make a 2% weight per volume ratio of alginate to media and stored in a refrigerator to maintain the integrity of the media.

For the first test, purified, sterile alginate hydrogels were made by mixing 1 mL of RGD-modified alginate with 340 µL of sterile concentrated calcium sulfate (2.1 g/mL) in 3 mL syringes for five seconds or ten mixes back and forth between syringes. The resulting slurry was ejected onto a glass plate and sandwiched between another glass plate at 2 mm in height. After letting the slurry sit for 20-30 minutes, the three gels were punched out in one quarter inch diameter shapes and placed into three different 15 mL centrifuge tubes. 10 mL of α-MEM was added to all of the tubes and each placed on a rotating plate set to run at 60 rpm for about 60 minutes. After the hour had elapsed, the centrifuge tubes were removed from the rotator, the media extracted from the tube, and new media placed in the tube and set back on the rotator. This was repeated at multiple times points in order to fully understand the degradation of the material. Over the two-week period in which this was conducted, there was a general trend of the pH towards a basic environment which makes sense given that the alginate has a multitude of alcohol and carboxylic acid groups throughout the polymer chain.

An additional preparation test was conducted incorporating cells into the system. Alginate was added to a syringe at 1.5 mL with 0.5 mL of MC3T3s at about 400,000 cells/mL. The syringe was mixed up and down to suspend the cells in solution. In another syringe, 680 µL of calcium sulfate was added, the two were connected with a syringe adaptor, and both were mixed back and forth for about five seconds or ten pumps in both directions. The solution was ejected, placed in-between glass plates at 2 mm in height, and allowed to sit for 20-30 minutes as was done in the earlier study. After the gel had set, ½ inch punches were taken out and placed in a 6 well plate along with 2 mL of α-MEM to each well. A baseline for the media was taken and observed at a pH of 7.85 and samples were taken every 2-3 days by completely removing the media from the wells, replacing with fresh, new media, and then taking the pH of the extracted

media. As the study progressed, the solution became more acidic over time as was expected from cell bioprocesses36.

The next step was to add the PCL pH nano-fiber to the system. For the nanofibers, 0.5 inch punches were made from the nano-fiber mat and placed on an ethanol bathed glass plate. A Kimwipe© wetted with ethanol was dabbed over the fibers, soaking and sterilizing them. The plate with the sterilized fibers was placed into the bio-fume hood in a sterile environment. Sterile alginate and calcium sulfate were also placed in the hood and the solution was prepared as earlier with the volumes changed to 1 mL for the alginate, 170 µL of calcium sulfate, and 0.5 mL of cell solution at 2 million cells/mL. The alginate and calcium solutions were mixed as was described previously and ejected on top of the fibers and placed between plates at a height of 0.8 mm. Gelation was allowed to occur for 20 minutes before 0.5 inch punches were taken over the fibers so that the gel and fiber were one stacked unit. The total system was moved into a 6 well plate with 2 mL of media in each well. After multiple attempts of this method, however, were unsuccessful as the gels and fibers continuously separated and provided inconclusive results. Another method of ejecting half of the alginate solution onto the glass plate, placing the nano-fiber, and then ejecting the remaining solution on top of the fiber was tested with limited success. Because of the fluid nature of the alginate solution before it starts gelation, the fibers were not held in the same place in the z-axis and which led to very complex and inconsistent measurements when the samples were imaged with the confocal microscope. To overcome the problems of the first two methods, a new method with, coverslips was tried.

The alginate solution, calcium solution, and the nanofibers were prepared as previously, with the exception that the nanofibers were punched out at 0.25 inches in diameter. Added to the system were 10 mm diameter coverslips, autoclaved for sterilization, and PBS and

polyethylenimine (PEI). Within the bio-fume hood, two different petri dishes were filled with PBS and PEI, respectively. The nano-fiber punches were placed in the PBS solution because the fibers are generally hydrophobic and the PBS would help in pre-soaking the fiber before exposing it to the extremely hydrated alginate gel. After letting the fibers sit for 10 minutes in the PBS solution, the glass was dipped in the PEI solution on one side so that the surface would readily bind to the hydrogel matrix [37]. The PEI coated glass was then transitioned over the other dish and a fiber was slid on top. The glass-fiber couple was then placed on top of a glass plate and allowed to dry for five minutes. An additional 10 µL of PEI was placed on and around the fiber on top of the glass in preparation for the hydrogel. Mixing of the hydrogel occurred the same as previously with 0.75 mL of alginate, 170 µL of calcium sulfate, and 0.25 mL of differing cell concentrations (0, 1, 5, and 10 million cells/mL). For the ejection step, about 150 µL of gelation solution was ejected on top of each of the different systems and sandwiched between two glass plates with a final gel height of 0.4 mm. The whole system was allowed to sit for 20 minutes in order for everything to fully form and solidify. The solidified glass, fiber, and gel were moved together as one unit into a 12 well plate and 0.5 mL of α-MEM was added to each well. The media was changed every 2-3 days and images were taken at the day 1 and day 7 points [18]. Data was collected using the confocal microscope. An attempt to collect quantitative data from the images using ImageJ did not give usable data and lead to a new direction using a plate reader instead of the confocal.

The best procedure ultimately was determined to be the below. For this final procedure, all materials used in the previous method were used (with the exception of PEI and PBS due to the system not needing them) with the addition of sterilized vacuum grease. In a 96 well plate, a small dab of sterilized vacuum grease was placed at the bottom of each of the wells and spread to

cover the bottom surface completely. Nanofibers were punched out in 6 mm diameter circles and sterilized in an ethanol bath as described previously. The nanofibers were transferred into the 96 well plates and placed on top of the grease to get a smooth surface and complete coverage of the fiber. The hydrogels were created as described before with two different setups using a standard containing no cells and another containing 0.7 million cells/mL of MC3T3s. The heights of the gels were 0.4 mm. Once gelation was complete, 6 mm diameter circles were punched out and were placed on top of the nanofibers in sets of 7 for each type of gel. In addition, 150 μL of α-MEM was added to each of the wells and the plate placed in the incubator. A reference row was added with HEPES, (4-(2-hydroxyethyl)-1-piperazineethanesulfonic acid), buffer solutions at pHs of 5, 6.5, 10.25, and 12 to serve as a standard curve for the other values. The plates were measured at the 1, 4, 6, 7, and 9 day marks at excitation and emission couples of 550 and 580 as well as 660 and 700, respectively, for the two dyes in solution (Octadecyl Rhodamine B Chloride and Chromoionophore II). The dye structures can be seen in Figure 10 and Figure 11 [38,39].

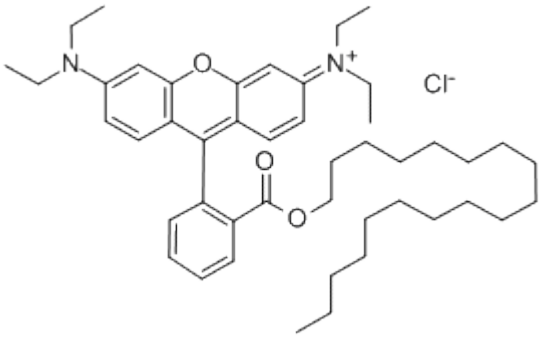

Figure 3.1 Chemical structure for Octadecyl Rhodamine B Chloride

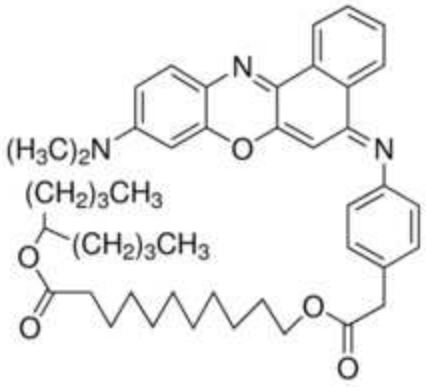

Figure 3.2 Chemical structure for Chromoionophore II

In order to simulate infection, on the 10th day the systems were in the 96 well plate, 30 µL of *E. coli* solution (10 million *E. coli* cells) was added to each of the wells. Fluorescence readings were taken right before the bacteria was added and at 3 and 19 hours after the bacteria had been added to the wells.

3.2 pH nanofibers Results and Discussion

Fluorescence values were collected from the plate reader with values given for the intensity of the different wave lengths at 585 and 700 nm with excitations at 550 and 660 nm, respectively. To calculate the α value, or the normalized value for the flourscence, a ratio was taken by dividing the 700 nm intensity by the 585 nm intensity denoted by the notation of R[S] where R stands for the ratio and S is the sample. From the standard curve that was created, an R[max] and R[min] value was created with the maximum being the pH of 5 and the minimum being the pH of 12. An α value was calculated from these using Equation 1.

$$\alpha = \frac{R[S] - R[min]}{R[max] - R[min]}$$

Equation 3.1 Equation used in determining the α value for normalizing the intensities of the samples on the plate reader.

This linear extrapolation method has been proven valid by others and is widely used in the field of biology [40,41]. A bar graph of the alpha values from the calibration curve was created and can be seen in Figure 12.

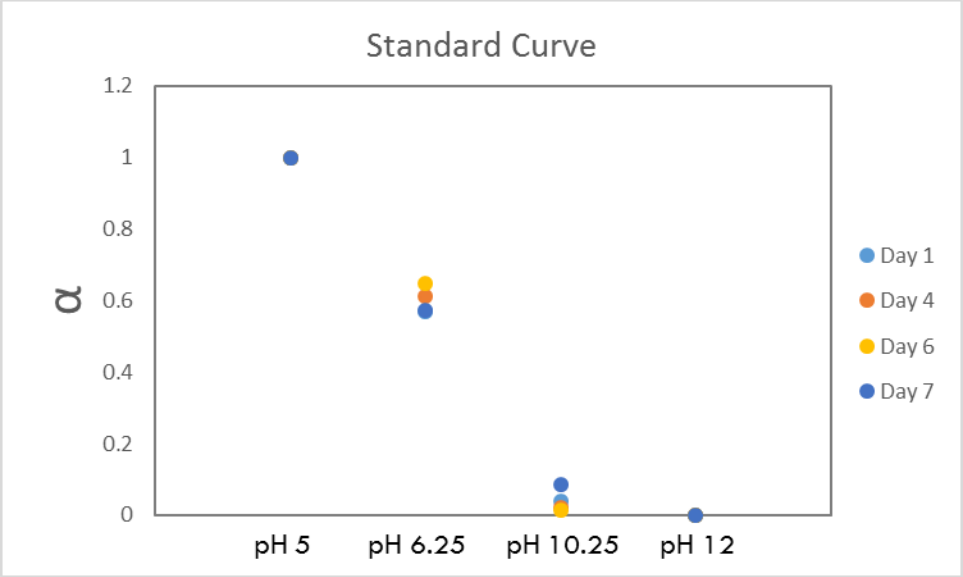

Figure 3.3 Calibration curve for the different HEPES buffers of pH 5, 6.25, 10.25, and 12.

After the α values were calculated, the average α value of each type of sample was determined as well as the standard deviation for each of the 5 time points for which there is data. A comparison between the blank system without any cells in it and the system that contained 0.7 million MC3T3 cells/mL was done, however, the blanks were too inconsistent so only the cell values are reported here. The data for the different days can be seen in Figure 13 and it is shown that the difference between the days 1 and 9 are statistically different from one another with a p-value of less than 0.06.

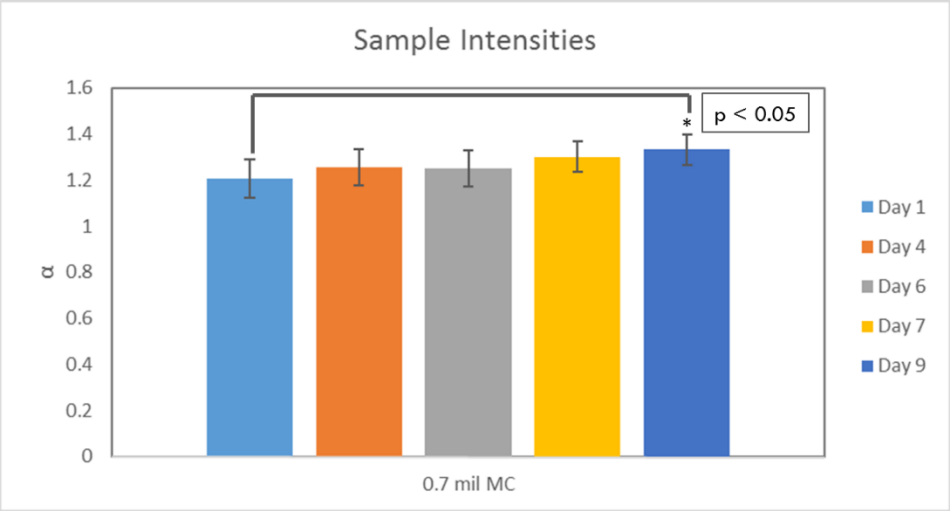

Figure 3.4 Relative α values for the blank sample of no cells to the 0.7 million MC3T3 cells/mL.

Along with bar graphs that report the average of the multiple samples within the set for each day and their respective standard deviation, a ANOVA test was run on all of the samples for each of the days with a p-value of 0.06 in order to determine statistical differences. The p-value of 0.06 correlates to a 95% confidence interval which means that the rejection or fail to reject can be said with 95% confidence. The null hypothesis was that each of the samples was statistically the same with an alternative hypothesis that each of the day's sample sets were statistically different from one another and if the p-value was greater than 0.06 then they would not be considered to be different from one another and on the flipped side, is the p-value less than 0.06 it will be considered to be statistically different from one another. Based on the p-values that were calculated for each of the sets in comparison to one another, only the Day 1 and Day 9 samples were statistically different from each other. The analytics for this information can be seen in Table 5.

Table 3.1 Statistical analysis for the ANOVA: One-way Analysis of Variance for the comparison between the set of data with and without cells.

One-way Analysis of Variance (ANOVA)								
The P value is 0.0604, considered not quite significant.								
Variation among column means is not significantly greater than expected by chance.								
Tukey-Kramer Multiple Comparisons Test								
If the value of q is greater than 4.155 then the P value is less than 0.05.								
Comparison					Mean Difference	q		P value
Column	A	vs	Column	B	-0.05057	1.67	ns	P>0.05
Column	A	vs	Column	C	-0.04545	1.501	ns	P>0.05
Column	A	vs	Column	D	-0.09542	3.15	ns	P>0.05
Column	A	vs	Column	E	-0.1267	4.184	*	P<0.05
Column	B	vs	Column	C	0.005118	0.169	ns	P>0.05
Column	B	vs	Column	D	-0.04485	1.481	ns	P>0.05
Column	B	vs	Column	E	-0.07614	2.514	ns	P>0.05
Column	C	vs	Column	D	-0.04996	1.65	ns	P>0.05
Column	C	vs	Column	E	-0.08126	2.683	ns	P>0.05
Column	D	vs	Column	E	-0.03129	1.033	ns	P>0.05

When looking at the data above, the trend does show that there is a general movement of increased values with a significant difference between day 1 and day 9, but the α values fall outside of the 0-1 range which would mean that the pH would fall outside of the standard curve between the pH range of 5-12. Based on the standard curve, this indicates the cells were in an environment that was more acidic that a pH of 5. Further work needs to be conducted to determine if this trend falls within the α value parameters of the standard curve. From this, we were able to determine that there were some changes but nothing that was note-worthy enough to determine a solid trend over time. Because of this, different areas were explored to provide more evidence.

To compliment the quantitative data from the plate reader, photos were taken with a confocal microscope. The confocal was set to take pictures at x10, at the High Quality image

value setting. In order to take the pictures, a set of coverslip, nano-fiber, and hydrogel with U251 cells at 5 million cells/mL was allowed to incubate along the same time scale as the 96 well plate for the previous results.

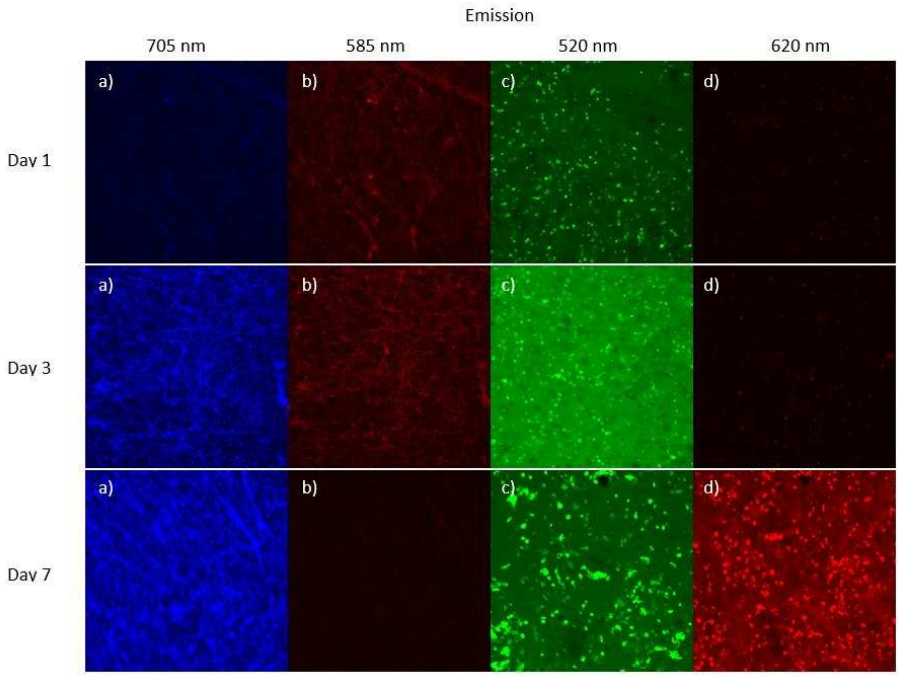

Figure 3.5 The emission images for the coverslip + nano-fiber + hydrogel system with 5 million U251 cells/mL at the time points of 1, 3, and 7 days (order of FRN, DS-Red2, FITC, and RN).

Images were taken at 1, 3, and 7 days after the initial start of incubation. For the images, four different excitations and emissions were taken using pre-programmed dye values, including FarRed-Narrow, DS-Red2, FITC, and Red-Narrow, in order to detect the 700 nm wavelength for the pH sensitive Chromoionophore II, the 585 nm wavelength to detect the normalization Octadecyl Rhodamine B Chloride, the 520 nm range to detect the live staining of cells, and the 620 nm range to detect the dead staining of cells, respectively. The Sensitivity and Laser values used were 32.0% and 5.0% for the DS-Red2, 65.0% and 80.0% for the FarRed-Narrow, 27.0% and 3.0% for the FITC, and 37.0% and 5.0% for the Red-Narrow for all images across each point

in time. The images of the three different time points are shown in Figure 14 in the order of FRN, DS-Red2, FITC, and RN.

In addition to the uniplanar pictures, the confocal images were stacked in the z direction and compressed into one 3D stack from which the cross-section of the photos was taken and is shown in Figure 15 for the three different days.

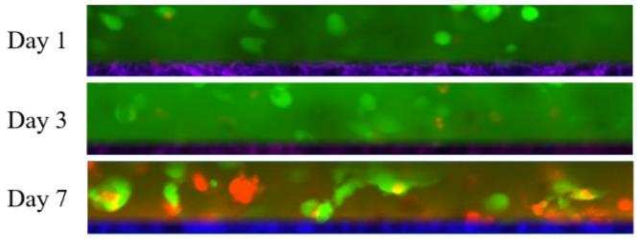

Figure 3.6 Z-stack of the confocal images take of the fiber + hydrogel system with U251 cells at days 1, 3, and 7.

Because MC3T3 cells were used in the testing for the nano-fiber response, additional pictures were taken of the system that included the nanofibers, hydrogel, and 1 million MC3T3 cells/mL (Figure 16, page 33). Additionally, z-stack images were taken of a system that contained 1 million MC3T3 cells/mL (Figure 17, page 33) at the 1, 4, and 7-day time points showing that cells are continuing to live in the system throughout the study.

Because there was not a huge shift observed with the cell systems, most likely due to the fact that the buffered media was maintaining a stable pH, *E. coli* was added so that the buffer could be broken and a pH shift might be detected. Time points were taken right before *E. coli* addition, at 3 hours, and at 19 hours after introduction to the system in order to simulate the early phases of infection on a system. The wells that the *E. coli* were added to were the same as the previously described study and included a blank with no cells and a sample with 0.7 million MC3T3 cells/mL at 10 days after the samples had been placed in the wells. The values for the *E. coli*

samples gave α values of 1.40 and 1.39 for the blank and cells wells respectively. At the 3-hour mark, the α values increased to 1.43 and 1.42 and continued to increase to 1.51 and 1.48 at 19 hours after introduction to the wells (Figure 18). Statistical analysis of the alpha values gave the below information. The null hypothesis for this data set was the three different time points are statistically the same. For this set of data, the 19-hour value had a p-value that showed it was statistically different from the No *E. coli* sample. All other data points were found to be statistically the same (Table 6).

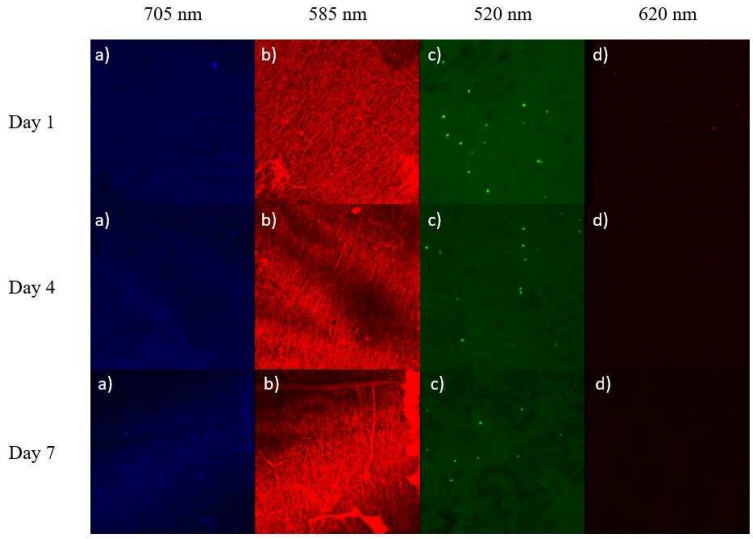

Figure 3.7 The emission images for the coverslip + nano-fiber + hydrogel system with 1 million MC3T3 cells/mL at the time points of 1 and 7 days.

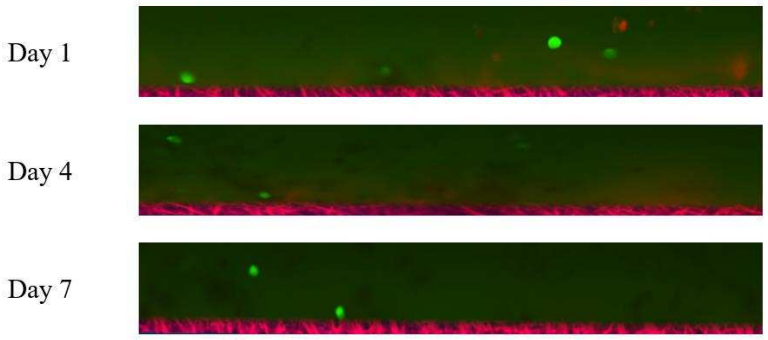

Figure 3.8 Z-stack of the confocal images take of the fiber + hydrogel system with MC3T3 cells at days 1, 4, and 7.

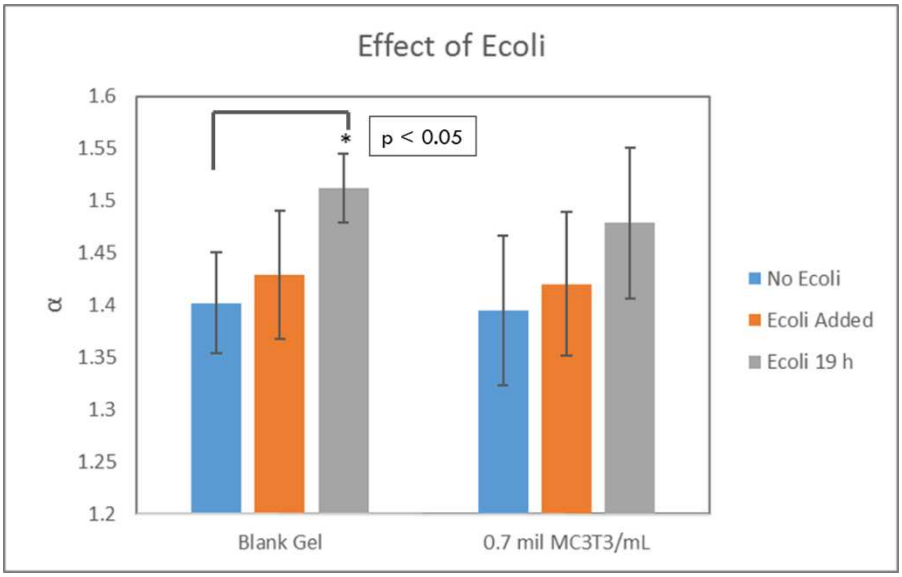

Figure 3.9 Showing the effect of *E. coli* added to a system and the subsequent pH shift that results from the infection. The * indicates that the value is significantly different from the base value of no E. coli.

Table 3.2 Statistical analysis for the ANOVA: One-way Analysis of Variance for the comparison between the set of data with and without cells within themselves to check for statistical difference.

One-way Analysis of Variance (ANOVA)					
No Cells					
The P value is 0.0280, considered not significant. Variation among column means is not significantly greater than expected by chance. Tukey-Kramer Multiple Comparisons Test *If the value of q is greater than 3.959 then the P value is less than 0.05.*					
Comparison		Difference	q		P value
Column A vs Column B		-0.02678	1.091	ns	P>0.05
Column A vs Column C		-0.11	4.482	*	P<0.05
Column B vs Column C		-0.08319	3.391	ns	P>0.05
Cells					
The P value is 0.1461, considered not significant. Variation among column means is not significantly greater than expected by chance. Tukey-Kramer Multiple Comparisons Test *If the value of q is greater than 3.674 then the P value is less than 0.05.*					
Comparison		Difference	q		P value
Column A vs Column B		-0.02534	0.8754	ns	P>0.05
Column A vs Column C		-0.08358	2.888	ns	P>0.05
Column B vs Column C		-0.05824	2.012	ns	P>0.05

As was seen with the α values for the MC3T3 cells, the values for the *E. coli* test also fell outside the 0-1 range of the standard curve even though there was a general trend towards a higher α value and a significant difference between hour 0 and 19 for the wells that contained MC3T3s.

To try and remedy the fact that the values were outside of the normalized range, the experiments were run again. To view the cell-laden hydrogels cultured on the NFSs, confocal images were obtained and are shown in Figure 19. Each row represents a different day of culturing, and each column represents a different wavelength observed. The first column (705 nm wavelength) was used to determine the pH of the system based on its fluorescence intensity. The relatively constant intensities of NFSs observed in Fig. 19 a,e,i indicated no observable changes in pH. The second column (585 nm wavelength, Fig. 19 b,f,j), which represents the relative density of the nanofibers, also appeared constant over time. The cells were shown to have high viability throughout the 7 days, with green cells present (Fig. 19 c,g,k) and very few dead cells (Fig. 19 d,h,l).

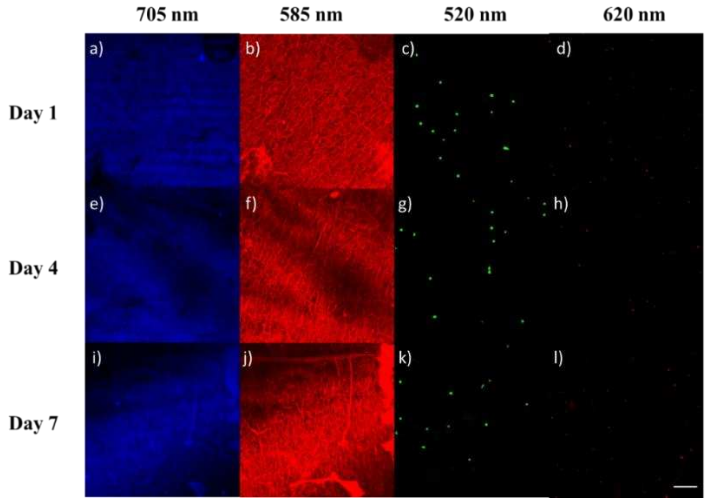

Figure 3.10 Grouping of confocal images taken at 1, 4, and 7 days of culture for the wavelengths labeled 705 nm for pH dependent fluorescence, 585 nm for fiber density, 520 nm for live cell staining, and 620 nm for dead cell staining. The scale bar represents 0.02 cm.

The fluorescence of the NFSs over time when cultured in the presence of both empty and cell-laden hydrogels was monitored in a high-throughput 96-well format with measurements obtained from a plate reader. The readings, reported as □-values, were stable over time (Figure 20) as expected within the buffered cell culture system. However, shortly after the addition of *E. coli* bacteria cells to these cultures, the □-values began to increase dramatically, reflecting a decrease of the pH of the system. There was significant variance between the samples due to variations in the system, such as nanofiber densities or exact placement of the nanofibers and hydrogels within the well, and thus the error bars are not displayed on this graph. However, the trend towards an increased α-value, and therefore decreased pH, is clear upon addition of the bacteria to the culture system.

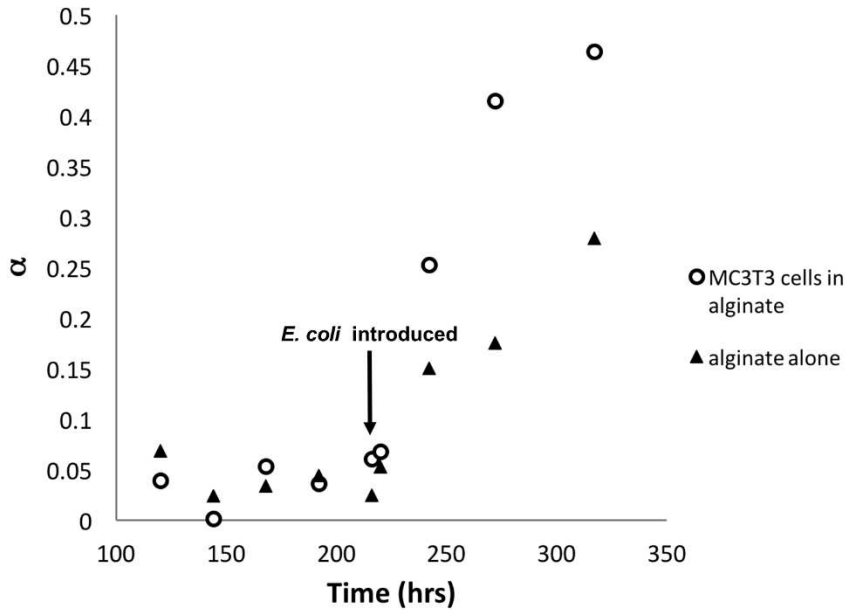

Figure 3.11 Scatter plot depicting the α-values for the systems with and without MC3T3s in the system. E. coli was added to the system at hour 216.

CHAPTER 4

CONCLUSION

The results from the bioglass project caused interest in what was happening with cells on the individual level. With the enzyme production levels and calcium deposition seen, it was expected that the cells would choose either the path of proliferation or differentiation. The coverslips were found to cause the cells to proceed down their differentiation pathway and become osteoblasts. The bioglass, however, maintained the cells in their pre-differentiated stated and allowed them to proliferate. Each of these pathways could have specific uses in prosthetics and could be used to manipulate the cells based on the desired outcome of the procedure. Because of these surprising and unexpected results, the process for which cellular studies are conducted came under question and a new method of microenvironment monitoring was studied using pH sensing nanofibers.

The ability to detect pH shifts in three dimensional cell culture conditions was examined. First, the ability to detect the fluorescence of the nanofibers when they were placed underneath empty or cell-laden hydrogels was confirmed. The fluorescence remains relatively constant over time, as expected within this buffered culture system with cells of high viability. This was also confirmed by quantitative measurements obtained for the system with a high throughput plate reader format, where the readings stayed relatively constant over time in culture. Cell culture media has a high buffering capacity to maintain the cell environment close to physiologic pH 7.4. To push the pH of the culturing system outside of its normal range, *E. coli* bacterial cells were added. These bacteria with a doubling time on the order of 30 minutes proliferate substantially faster than mammalian cells and rapidly overwhelm the culture system, depleting

nutrients and decreasing the pH. Indeed, the NFSs were readily able to detect this decrease in pH. These results demonstrate that these NFSs are promising tools for the detection of pH shifts that may influence cellular environments. Furthermore, a high throughput format for rapid screening of various culture conditions may be utilized.

4.1 Recommendations for Further Work

In future work for these projects, there are three areas that need to be looked at more closely: calcium leaking from the bioglass, the fibers, and the cells. An in depth study needs to be performed on the bioglass material to determine if there is calcium leaching from the glass and what effects that is having on the cells. For the fibers, a new method of observation needs to be determined so that more precise measurements can be taken of the fluorescence and consequently tighter error. For the cells, a wider variety of cells needs to be observed in order to determine if the types of cells would cause a shift in the pH values that would be able to be detected by the system. If was shown that the pre-osteoblasts were not able to provide any data as to a shift in their own pH, but, when the bacteria were added to the system the buffer in the media was overcome and the shift was able to be seen in the α values. Additionally, varying concentrations of the cells should be used in order to determine if the fiber system is able to detect the quantitative number of cells.

REFERENCES

(1) Xiantao, W., Martindale, J. L., and Yusen, L. (1998) The cellular response to oxidative stress: influences of mitogen-activated protein kinase signalling pathways on cell survival. *Biochemical*

(2) Johnston, J. A., Ward, C. L., and Kopito, R. R. (1998) Aggresomes: a cellular response to misfolded proteins. *The Journal of cell biology*.

(3) Cornejo, I. A. (2014) Hidden treasures: Turning food waste into glass. *American Ceramic Society Bulletin 93*, 24–27.

(4) Wang, D., Christensen, K., and Chawla, K. (1999) Isolation and characterization of MC3T3-E1 preosteoblast subclones with distinct in vitro and in vivo differentiation/mineralization potential. *Journal of Bone and …*.

(5) Krebs, M. D., Salter, E., Chen, E., and Sutter, K. A. (2010) Calcium phosphate-DNA nanoparticle gene delivery from alginate hydrogels induces in vivo osteogenesis. *Journal of Biomedical …*.

(6) Dubach, J. M., Harjes, D. I., and Clark, H. A. (2007) Fluorescent ion-selective nanosensors for intracellular analysis with improved lifetime and size. *Nano Letters 7*, 1827.

(7) Pickover, C. A. (2012) The Medical Book: From Witch Doctors to Robot Surgeons: 250 Milestones in the History of Medicine.

(8) Smidsrød, O., and Skja, G. (1990) Alginate as immobilization matrix for cells. *Trends in biotechnology*.

(9) Lian, J. B., and Stein, G. S. (1992) Concepts of osteoblast growth and differentiation: basis for modulation of bone cell development and tissue formation. *Critical Reviews in Oral Biology & Medicine*.

(10) Anderson, J. M., Rodriguez, A., and Chang, D. T. (2008) Foreign body reaction to biomaterials. *Seminars in immunology*.

(11) Torres, M. R., Sousa, A., Filho, E. S., and Melo, D. F. (2007) Extraction and physicochemical characterization of Sargassum vulgare alginate from Brazil. *Carbohydrate …*.

(12) Kuo, C. K., and Ma, P. X. (2001) Ionically crosslinked alginate hydrogels as scaffolds for tissue engineering: part 1. Structure, gelation rate and mechanical properties. *Biomaterials*.

(13) Physically crosslinked alginate/N,O-carboxymethyl chitosan hydrogels with calcium for oral delivery of protein drugs. *Biomaterials*.

(14) . (2012) The influence of mixing methods and disinfectant on the physical properties of alginate impression materials. *The European Journal of Orthodontics 35*, 381.

(15) Hoffman, A. S., and Hoffman, A. S. Hydrogels for biomedical applications ☆. *Advanced drug delivery reviews*.

(16) Häggström, M. Blood values sorted by mass and molar concentration.

(17) Alginate hydrogels as synthetic extracellular matrix materials.

(18) Takuwa, Y., Ohse, C., Wang, E. A., and Wozney, J. M. (1991) Bone morphogenetic protein-2 stimulates alkaline phosphatase activity and collagen synthesis in cultured osteoblastic cells, MC3T3-E1. *Biochemical and …*.

(19) Cornejo, I. A., Reimanis, I. E., and Ramalingam, S. US Patent Application: Methods of Making Glass from Organic Waste Food Streams.

(20) Hench, L. L. (2006) The story of Bioglass. *J Mater Sci Mater Med 17*, 967–978.

(21) Miniature Sodium-Selective Ion-Exchange Optode with Fluorescent pH Chromoionophores and Tunable Dynamic Range.

(22) Cash, K. J., and Clark, H. A. (2010) Nanosensors and nanomaterials for monitoring glucose in diabetes. *Trends in molecular medicine*.

(23) Cash, K. J., and Clark, H. A. (2013) Phosphorescent nanosensors for in vivo tracking of histamine levels. *Analytical chemistry*.

(24) Cash, K. J., and Clark, H. A. (2010) Nanosensors and nanomaterials for monitoring glucose in diabetes. *Trends in molecular medicine*.

(25) submit version of pH paper .docx.

(26) Castano-Izquierdo, H., Alvarez-Barreto, J., van den Dolder, J., Jansen, J. A., Mikos, A. G., and Sikavitsas, V. I. (2007) Pre-culture period of mesenchymal stem cells in osteogenic media influences their in vivo bone forming potential. *J Biomed Mater Res A 82*, 129–138.

(27) Tice, R., and Vasquez, M. (1998) Protocol for the application of the pH> 13 alkaline single cell gel (SCG) assay to the detection of DNA damage in mammalian cells. *Sigma (x-100).*

(28) Baksh, D., Yao, R., and Tuan, R. S. (2007) Comparison of proliferative and multilineage differentiation potential of human mesenchymal stem cells derived from umbilical cord and bone marrow. *Stem Cells 25*, 1384–1392.

(29) Beck, G. R., Sullivan, E. C., Moran, E., and Zerler, B. (1998) Relationship between alkaline phosphatase levels, osteopontin expression, and mineralization in differentiating MC3T3-E1 osteoblasts. *J Cell Biochem 68*, 269–280.

(30) Yamaguchi, T., Chattopadhyay, N., Kifor, O., Butters, R. R., Sugimoto, T., and Brown, E. M. (1998) Mouse osteoblastic cell line (MC3T3-E1) expresses extracellular calcium (Ca2+o)-sensing receptor and its agonists stimulate chemotaxis and proliferation of MC3T3-E1 cells. *J Bone Miner Res 13*, 1530–1538.

(31) BioVision. Calcium Colorimetric Assay Kit.

(32) Ahn, S. J., Costa, J., and Emanuel, J. R. (1996) PicoGreen quantitation of DNA: effective evaluation of samples pre-or psost-PCR. *Nucleic acids research*.

(33) . (1976) Regulation of Calcium Metabolism. *Annals of Clinical Biochemistry: An international journal of biochemistry and laboratory medicine 13*, 518.

(34) Owen, T. A., Aronow, M., Shalhoub, V., Barone, L. M., Wilming, L., Tassinari, M. S., Kennedy, M. B., Pockwinse, S., Lian, J. B., and Stein, G. S. (1990) Progressive development of the rat osteoblast phenotype in vitro: reciprocal relationships in expression of genes associated with osteoblast proliferation and differentiation during formation of the bone extracellular matrix. *Journal of cellular physiology 143*, 420–430.

(35) Mata, E., Igartua, M., Patarroyo, M. E., Pedraz, J. L., and Hernández, R. M. (2011) Enhancing immunogenicity to PLGA microparticulate systems by incorporation of alginate and RGD-modified alginate. *Eur J Pharm Sci 44*, 32–40.

(36) Lazáry, A., Balla, B., Kósa, J. P., Bácsi, K., Nagy, Z., Takács, I., Varga, P. P., Speer, G., and Lakatos, P. (2006) Effect of gypsum on proliferation and differentiation of MC3T3-E1 mouse osteoblastic cells. *Biomaterials 28*, 393–399.

(37) Halder, A., Maiti, S., and Sa, B. (2005) Entrapment efficiency and release characteristics of polyethyleneimine-treated or -untreated calcium alginate beads loaded with propranolol-resin complex. *Int J Pharm 302*, 84–94.

(38) Hoekstra, D., de Boer, T., Klappe, K., and Wilschut, J. (1984) Fluorescence method for measuring the kinetics of fusion between biological membranes. *Biochemistry 23*, 5675–5681.

(39) He, H., Mortellaro, M. A., Leiner, M. J. P., Young, S. T., Fraatz, R. J., and Tusa, J. K. (2003) A fluorescent chemosensor for sodium based on photoinduced electron transfer. *Analytical chemistry 75*, 549–555.

(40) Pace, C. N., and Shaw, K. L. (2000) Linear extrapolation method of analyzing solvent denaturation curves. *Proteins Suppl 4*, 1–7.

(41) Bolen, D. W., and Santoro, M. M. (1988) Unfolding free energy changes determined by the linear extrapolation method. 2. Incorporation of. DELTA. G. degree. NU values in a thermodynamic cycle. *Biochemistry*.